BBA - Molecular Basis of Disease 1865 (2019) 2342–2355

Contents lists available at ScienceDirect

BBA - Molecular Basis of Disease

journal homepage: www.elsevier.com/locate/bbadis

Impaired renal organic anion transport 1 (SLC22A6) and its regulation following acute myocardial infarction and reperfusion injury in rats

Kungsadal Sirijariyawat[a], Atcharaporn Ontawong[a,b], Siripong Palee[c], Savitree Thummasorn[c], Chayodom Maneechote[c], Oranit Boonphang[a], Varanuj Chatsudthipong[d], Nipon Chattipakorn[a,c], Chutima Srimaroeng[a,*]

[a] Department of Physiology, Faculty of Medicine, Chiang Mai University, Chiang Mai, Thailand
[b] Division of Physiology, School of Medical Sciences, University of Phayao, Phayao, Thailand
[c] Cardiac Electrophysiology Research and Training Center, Faculty of Medicine, Chiang Mai University, Chiang Mai, Thailand
[d] Research Center of Transport Protein for Medical Innovation, Faculty of Science, Mahidol University, Bangkok, Thailand

ARTICLE INFO

Keywords:
Organic anion transporter 1
Organic anion transporter 3
Acute kidney injury
Acute myocardial ischemia and reperfusion
Mitochondrial dysfunction
Oxidative stress

ABSTRACT

Acute kidney injury (AKI) is a high frequent and common complication following acute myocardial infarction (AMI). This study examined and identified the effect of AMI-induced AKI on organic anion transporter 1 (Oat1) and Oat3 transport using clinical setting of pre-renal AKI in vivo. Cardiac ischaemia (CI) and cardiac ischaemia and reperfusion (CIR) were induced in rats by 30-min left anterior descending coronary artery occlusion and 30-min occlusion followed by 120-min reperfusion, respectively. Renal hemodynamic parameters, mitochondrial function and Oat1/Oat3 expression and function were determined along with biochemical markers. Results showed that CI markedly reduced renal blood flow and pressure by approximately 40%, while these parameters were recovered during reperfusion. CI and CIR progressively attenuated renal function and induced oxidative stress by increasing plasma BUN, creatinine and malondialdehyde levels. Correspondingly, SOD, GPx, CAT mRNAs were decreased, while TNFα, IL1β, COX2, iNOS, NOX2, NOX4, and xanthine oxidase were increased. Mitochondrial dysfunction as indicated by increasing ROS, membrane depolarisation, swelling and caspase3 activation were shown. Early significant detection of AKI; KIM1, IL18, was found. All of which deteriorated *para*-aminohippurate transport by down-regulating Oat1 during sudden ischaemia. This consequent blunted the trafficking rate of Oat1/Oat3 transport via down-regulating PKCζ/Akt and up-regulating PKCα/NFκB during CI and CIR. Thus, this promising study indicates that CI and CIR abruptly impaired renal Oat1 and regulatory proteins of Oat1/Oat3, which supports dysregulation of remote sensing and signalling and inter-organ/organismal communication. Oat1, therefore, could potentially worsen AKI and might be a potential therapeutic target for early reversal of such injury.

1. Introduction

Acute kidney injury (AKI) is frequently associated and defined to be a common complication following acute myocardial infarction (AMI) due to transient episodes of ischaemia (hypoperfusion) and reperfusion [1]. At present, the prevalence of AKI after AMI remains high with a broad range of 5–59%, depending upon AKI definition and clinical characteristics [1,2], which persist due to failure of preventive strategies leading to rising in-hospital mortality. Previous studies demonstrate that cardiac and renal ischaemia and reperfusion (I/R) share common pathophysiological mechanisms causing severe cellular injuries, which lead to organ dysfunctions and are believed to be multifactorial [2]. During renal I/R condition, the reperfusion itself causes severe cellular injury leading to AKI and renal dysfunction [3]. Renal hemodynamic alteration, nitric oxide production, inflammation and oxidative stress have been proposed to play as major mediators of

Abbreviations: Oat1, organic anion transporter 1; Oat3, organic anion transporter 3; CI, cardiac ischaemia; CIR, cardiac ischaemia and reperfusion; SOD, superoxide dismutase; GPx, glutathione peroxidase; CAT, catalase; TNFα, tumour necrosis factor alpha; IL1β, interleukin 1 beta; COX2, cyclooxygenase 2; iNOS, inducible nitric oxide; NOX2, NAPDH oxidase2; NOX4, NAPDH oxidase4; KIM1, kidney injury molecule 1; IL18, interleukin 18; PKCζ, protein kinase zeta; Akt, protein kinase B; PKCα, protein kinase alpha; NFκB, nuclear transcription factor kappa b

* Corresponding author at: Department of Physiology, Faculty of Medicine, Chiang Mai University, 110 Intavaroros Rd., Sri-phum district, Muang, Chiangmai 50200, Thailand.
E-mail address: chutima.srimaroeng@cmu.ac.th (C. Srimaroeng).

https://doi.org/10.1016/j.bbadis.2019.05.013
Received 6 February 2019; Received in revised form 6 May 2019; Accepted 19 May 2019
Available online 21 May 2019
0925-4439/

worsening glomerular and tubular structures after renal I/R [4]. Thus, understanding the multifactorial mechanisms involved in AKI after AMI is crucially required to seek potential targets for early intervention.

Renal proximal tubules play an important role in the elimination of several xenobiotics, including endogenous metabolites, drugs and toxins [5]. The active secretion of organic substances to the tubular lumen appears to be restricted to the basolateral membrane of proximal tubule via several transporters. Among these, organic anion transporters 1 (Oat1) and 3 (Oat3) play a significant role in rate-limiting basolateral uptake of organic anions due to their high expression using tertiary active transport process [5–7]. These two transporters initially uptake anionic substrates from blood circulation into the renal epithelial cells against an electrochemical gradient in exchanging for the efflux of alpha-ketoglutarate (α-KG). The outwardly directed gradient for α-KG is not only maintained by intracellular metabolic generation of α-KG through mitochondrial Kreb's cycle activity, but also is fuelled by active α-KG uptake across the basolateral membrane via a sodium dicarboxylate cotransporter. Na^+ gradient is, in turn, driven by utilising primary active Na^+/K^+ ATPase [5–7]. The two transporters recognise a broad spectrum of substrates including *para*-aminohippurate (PAH), ochratoxin A and uremic toxins, whereas estrone sulphate (ES) is only specific for Oat3 [5–7]. More recently, Oat1 was suggested to be the centered-network which plays a key role in remote sensing and signalling hypothesis by modulating essential metabolites. This includes kreb's cycle intermediates, enterobiome-metabolites, mainly indoxyle sulphate, and key signalling molecules including prostagladins, polyamines and cyclic nucleotides using a novel multi-tiered systems biology approach [8]. Furthermore, previous studies reported that uremic toxins produced from organ dysfunction, including hippurate and indoleacetate, are transported by Oat1, while Oat3 was responsible for handling 3-carboxy-4-methyl-5-propyl-2-furanpropionate. Additionally, both Oat1 and Oat3 equally contributed to the transport of indoxyl sulphate (IS) [9–12]. Subsequently, plasma endogenous anionic metabolites produced in Oat1 knockout mice including indoxyl sulphate, kynurenine, and xanthurenic acid as well as the predicted CAS 5435-73-4 pharmacophore were identified using *en mass* untargeted metabolomics [13]. These data strongly indicate that Oat1 and Oat3, particularly the former, play a crucial role in the deterioration of kidney transport function by accumulation of uremic toxins derived from organ dysfunction. The lack of the ability of Oats-mediated to communication between organs and/or organisms has recently been emphasised to be a key of dyshomeostasis in uraemic syndrome of chronic kidney disease [14]. Thus, any changes in basolateral renal transporters, Oat1 and Oat3, could also potentially affect the clearance of such uremic toxins, resulting in ineffective treatment for AKI.

Previous study showed the reduction of Oat1 expression with a decrease of renal organic anion secretion in chronic renal failure in rats [15]. In addition, an increase in IS in proximal tubular cells up-regulated Oat1 and Oat3 in chronic renal failure [16], while bilateral urethral obstruction and renal I/R injury in rats decreased mRNA and protein expressions of both Oat1 and Oat3 [17,18]. Previous study also found that renal uptake of benzylpenicillin, substrates for Oat1 and Oat3, was decreased, as caused by down-regulating the expression of these two transporters in adenine-induced chronic renal failure (CRF) in rats [19]. Likewise, human OAT1 and OAT3 were down-regulated in CRF, leading to impaired renal secretion of cytotoxic metabolites, such as cefazolin and phenolsulfonphthalein and glutarate derivatives, such as α-KG, L-2OHGA, D-2OHGA, 3OHGA, glutaconate and adipate, resulting in mitochondrial dysfunction and nephrotoxicity [20]. Recently, prostaglandin E2 down-regulated rat renal Oat1 and Oat3 expression and function after a 24-h induced renal I/R injury; in addition, the Oat inhibitor probenecid was able to protect against renal damage, suggesting a role of renal Oats in AKI [21]. The role of Oat1 protected mercury-induced kidney injury was also been demonstrated in Oat1 knockout mice, suggesting that Oat1 might be an effective therapeutic target for prevention of kidney injury [22]. In addition, acute uraemia-induced by in vivo pre-renal, nephrotoxic, and post-renal AKI models has demonstrated a positive correlation among plasma urea and the decrease in functional Oat1 and Oat3 expressions on plasma membrane [23]. Our previous study demonstrated that Oat1 and Oat3 share a common trafficking process through insulin signalling [24]. The oxidative stress induced by hyperglycaemia also impaired the regulatory function of these transporters, by associating with the activation of PKCα/NFκB and deactivation of PKCζ [25]. Hence, we hypothesised that CI and CIR could induce systemic and renal oxidative stresses, leading to impaired renal basolateral Oats function and their regulatory proteins, which could potentially worsen AKI after AMI. These consequences could support the hypotheses of remote sensing signalling and communication between organs and organisms. Finding such an early window of opportunity might be the promising target for successful therapeutic intervention in AKI.

2. Materials and methods

2.1. Chemicals

CelLytic MT mammalian tissue lysis/extraction reagent, unlabelled estrone sulphate (ES), *para*-aminohippurate (PAH) and 2,3,5-triphenyltetrazolium chloride were purchased from Sigma Aldrich (St. Louise, MO, USA). Polyclonal rabbit anti-rOat1 and monoclonal mouse anti-β-actin antibodies were purchased from Abcam (Cambridge, MA, USA), while polyclonal rabbit anti-rOat3 antibody was obtained from Cosmobio (Tokyo, Japan). Polyclonal rabbit anti-PKC, phosphorylated PKCα (p-PKCα), p65 subunit of NFκB (p65NFκB), goat anti-mouse and rabbit IgG horseradish peroxidase-conjugated secondary antibodies were purchased from Santa Cruz (Santa Cruz, CA, USA). Monoclonal mouse anti-lamin B1 and polyclonal rabbit anti-phosphorylated PKCζ (p-PKCζ) were purchased from Cell Signalling (Danvers, MA, USA). Polyclonal rabbit anti-PKCζ antibody was obtained from Invitrogen (Carlsbad, CA, USA). Monoclonal mouse anti-Na^+-K^+-ATPase was obtained from Novus Biologicals (Littleton, CO, USA). [^{3}H]-ES (specific activity: SA 50 Ci/mmol) and [^{3}H]-PAH (SA 1 Ci/mmol) were purchased from Perkin Elmer (Waltham, MA, USA). Insulin was obtained from Biocon (Bangkok, Thailand) and complete protease inhibitor cocktail was purchased from Roche Applied Science (Indianapolis, IN, USA). Thiobarbituric acid reactive substances (TBARS) assay was purchased from Cayman Chemical (MI, USA). Zoletil was purchased from Virbac Laboratories (Carros, France) while xylazine was obtained from Laboratorios Calier (Barcelona, Spain). All other chemicals with high purity were obtained from commercial sources.

2.2. Animals

Adult male Wistar rats weighing 300–350 g were obtained from the Nomura Siam International (Bangkok, Thailand). The animal facilities and protocols were approved by the Laboratory Animal Care and Use Committee at Faculty of Medicine, Chiang Mai University, Chiang Mai, Thailand (Protocol no 7/2559). All experimental animals were housed in a room and maintained at 25 ± 1 °C on a 12:12 h dark-light cycle, and allowed to acclimatise at least 1 week before the beginning of the experiments. The rats were randomly divided into sham, cardiac ischaemia alone (CI) and cardiac ischaemia and reperfusion (CIR) groups. Before experiments, rats were fasted overnight with free access to water.

2.2.1. Cardiac ischaemia and cardiac ischaemia and reperfusion injury protocol

CI and CIR injury protocol were performed according to previous studies [26]. Briefly, rats were weighed and anaesthetised using 50 mg/kg zoletil and 0.15 mg/kg xylazine, intramuscularly. Tracheostomy was performed and rats were ventilated with room air from a positive pressure rodent ventilator (CWE Inc., Ardmore, Pennsylvania, USA).

Lead II electrocardiography (ECG) was recorded throughout the experiment. A left-side thoracotomy was performed at the fourth intercostal space, and the pericardium was incised to expose the heart. Left anterior descending (LAD) coronary artery was then identified and ligated at approximately 2 mm distal to its origin. The end of a ligature was passed through a small vinyl tube which is used to occlude the LAD by pulling the thread for 30 min in the CI group, while the addition of a 120-min reperfusion was performed in the CIR group. ST elevation from ECG was used to confirm ischaemia. At the end of study, the animals were sacrificed and the blood, heart, kidney and spot urine were collected for subsequent experiments. Kidney index was calculated by kidney weight per body weight and multiplied by 1000. For infarct size determination, the heart was excised and mounted on the modified Langendorff apparatus via the aorta after the end of experiment. Cold saline solution was used to flush out the blood, after which the LAD was re-occluded and 1 mL of 0.5% (w/v) Evans blue dye was injected to define the area at risk. Evans blue dye stained the perfused myocardium, whereas the LAD occlusion area did not stain with the dye. Subsequently, the heart was sliced into pieces of approximately 1 mm thickness and incubated with 1% buffered 2,3,5-triphenyltetrazolium chloride, followed by placing the pieces in 10% formalin overnight. The infarct and remote areas were determined as previously described [26].

2.2.2. Determination of renal blood flow and renal perfusion pressure

The non-invasive flow and pressure assessment of the right renal artery were carried out using slightly modified protocol of pulsed wave viewed ultrasound system, with centre frequency of 8 MHz as previously described [27]. The rats were in supine on the platform, positioned towards the ultrasound probe. Transverse image of the right kidney was defined, and the flow through the right renal artery was measured in directionality to renal blood flow and renal perfusion pressure at baseline, 15 min after ischaemia and 15 min before end of reperfusion. The renal arterial flow velocity was recorded and presented as meter/s (m/s), while renal perfusion pressure was reported as percent relative to baseline.

2.3. Biochemical parameters

The quantitative total blood urea nitrogen (BUN), plasma creatinine and urine creatinine were determined by commercial enzymatic colorimetric assays (Erba Lachema, Brno, Czech Republic). Plasma malondialdehyde (MDA) was determined using commercial TBARS assay kit (Cayman Chemical, Ann Arbor, MI, USA).

2.4. Measurement of total malondialdehyde level in renal cortical tissues

To determine renal oxidative stress, the measurement of total renal cortical malondialdehyde (MDA) level was performed. Briefly, renal cortical tissues were cut and suspended in lytic buffer containing protease inhibitors according to the manufacturer's protocol. The tissues were then homogenised and centrifuged at 2500 $\times g$ for 10 min at 4 °C and supernatant was collected for determination of MDA level as mentioned above. Each sample was expressed as total MDA level to total protein concentration (nmol/mg protein).

2.5. Renal histological examination

To assess renal morphology, the kidney was excised and one-half of the kidney was fixed in 4% neutral formalin buffer for 12–24 h and embedded in paraffin. Each slide was cut into 5–7 μm thick sections and subsequently stained with haematoxylin and eosin (H&E). The lesions were confirmed by periodic acid-Schiff base (PAS) as previously described [28]. The tissue morphological change was determined using bright-field microscopic evaluation. The morphological analysis of glomerular size, mesangial matrix and tubular lesions was assessed semi-quantitatively. The pathological severity was graded as mild, moderate and severe. Renal tubular and mitochondrial morphology were assessed by fixing renal cortical tissues with 2.5% glutaraldehyde in 0.1 M phosphate buffer overnight, and post-fixed with 1% cacodylate-buffered osmium tetroxide for 2 h at room temperature. Subsequently, the renal tissue and mitochondria were dehydrated with graded series of ethanol, embedded and cut. Renal tubular and mitochondrial morphology were determined using a transmission electron microscope.

2.6. Renal slice preparation and transport study

Rat kidneys were removed and placed in oxygenated saline buffer, and renal cortical slices ($\leq$0.5 mm; 5–15 mg, wet weight) were cut with a Stadie-Riggs microtome and maintained in ice-cold oxygenated modified Cross and Taggart buffer containing (mM): 95 NaCl, 80 mannitol, 5 KCl, 0.74 $CaCl_2$ and 9.5 Na_2HPO_4, pH 7.4. The slices were incubated in modified Cross and Taggart buffer containing either 5 μM [^{3}H]-PAH or 100 nM [^{3}H]-ES for 30 min. For determination of the trafficking process of Oat1 and Oat3, the slices were pre-incubated in the absence or presence of 30 μg/mL insulin in the buffer, followed by either 5 μM [^{3}H]-PAH or 50 nM of [^{3}H]-ES for another 30 min. Uptake was stopped by adding 1 mL of ice-cold buffer. Slices were washed, blotted, weighed and dissolved in 1 N NaOH and neutralised with 1 N HCl. Scintillation fluid was added and the radioactivity was quantified using a Liquid Scintillation Analyzer (PerkinElmer Life Sciences, MA, USA). Uptakes of radiolabelled substrates were calculated as tissue to medium (T/M) ratio, i.e. (DPM/mg) tissue/(DPM/μl) medium.

2.7. Renal mitochondrial isolation and function

2.7.1. Mitochondrial isolation protocol

Renal mitochondrial isolation protocol was modified and carried out as previously described [29,30]. Briefly, the renal cortical tissues were cut into small pieces and homogenised in ice-cold isolation buffer containing (mM): 215 mannitol, 75 sucrose, 1 EGTA, 20 HEPES and 0.1% BSA, pH 7.2, and centrifuged at 3700 rpm for 8 min at 4 °C. The supernatant was collected and re-centrifuged at 11,800 rpm for 10 min at 4 °C. The pellet from this step was re-suspended in ice-cold isolation buffer, and the sample was layered on 15% percoll. The sample was centrifuged at 15,400 rpm for 9 min at 4 °C, and the pellet was re-suspended in the same buffer and re-centrifuged at 15,400 rpm for 13 min at 4 °C to remove percoll. The pellet was then re-suspended in ice-cold mitochondrial buffer containing (mM): 215 mannitol, 75 sucrose, 20 HEPES, and 0.1% BSA, pH 7.2 and centrifuged at 11,800 rpm for 13 min at 4 °C. The pellet from this step was designated as the mitochondrial fraction and used for further experiments.

2.7.2. Determination of renal mitochondrial swelling, reactive oxygen species and membrane depolarisation

For determination of renal mitochondrial swelling, isolated renal mitochondria was incubated in respiration buffer containing (mM): 100 KCl, 10 HEPES and 5 KH_2PO_4 as modified by previous study [31,32]. The absorbance at 540 nm was determined using Synergy™ HT microplate reader (Biotek, VT). A decrease in absorbance represents mitochondrial swelling. The level of reactive oxygen species (ROS) in isolated renal cortical mitochondria was determined by modifying from previous study [31,32]. Briefly, mitochondria was incubated in phosphate buffer saline (PBS) containing 10 μM H_2DCFDA at 37 °C for 30 min. Excess dye was aspirated and mitochondria was washed three times by PBS. The fluorescence intensity of dichlorofluorescein (DCF) was subsequently determined at 485 nm excitation and 528 nm emission using Synergy™ HT microplate reader (Biotek, VT). Renal mitochondrial membrane depolarisation was also assessed using JC-1 dye (Calbiochem, Darmstadt, Germany), as modified by previous study [31,32]. The isolated renal cortical mitochondria was incubated with 10 μM JC-1 for 30 min at 37 °C. Excess JC-1 dye was removed by PBS

Table 1
Primer sequences and expected amplicon sizes for the gene amplification.

cDNA	Genbank acc. no.	Forward primer	Reverse primer	Amplicon size (bp)
Mn SOD	NM017051.2	ACGCGACCTACGTGAACAATCT	CAGTGCAGGCTGAAGAGCAA	101
Cu-Zn SOD	X05634	GCAGAAGGCAAGCGGTGAAC	TAGCAGGACAGC AGATGAGT	387
GPx	NM030826	CTCTCCGCGGTG GCACAGT	CCACCACCGGGT CGGACATAC	297
CAT	NM012520	ACAACTCCCAGA AGCCTAAGAATG	GCTTTTCCCTTG GCAGCTATG	76
TNFα	NM012675.3	CCCAAAGGGAAGAGAAGTTC	CCACTTGGTGGTTTGCTACA	132
IL-1β	NM031512.2	GTGATGTTCCCATTAGACAGC	CTTTCATCACACAGGACAGG	228
iNOS	NM012611.3	GACCAGAAACTGTCTCACCTG	CGAACATCGAACGTCTCACA	137
NOX2	NM023965.1	CAATTCACACCATTGCACATC	CGAGTCACAGCCACATACAG	181
NOX4	NM053524.1	TCCATCAAGCCAAGATTCTGAG	GGTTTCCAGTCATCCAGTAGAG	192
XO	NM017154.1	TGCCAGACCATACTGAAAAGG	AAGCCACCCCATAACTGAAAT	196
β-actin	NM031144	ATGGTGGGTA TGGGTCAGAA	GGGGTGTTGAAG GTCTCAAA	241

Mn SOD: manganese superoxide dismutase, Cu-Zn SOD: copper zinc superoxide dismutase, GPx: glutathione peroxidase, CAT: catalase, TNF-α: tumour necrosis factor alpha, IL-1β: interleukin-1 beta, iNOS: inducible nitric oxide synthase, NOX2: NADPH oxidases 2, NOX4: NADPH oxidases 4, XO: xanthine oxidase, β-actin: beta-actin.

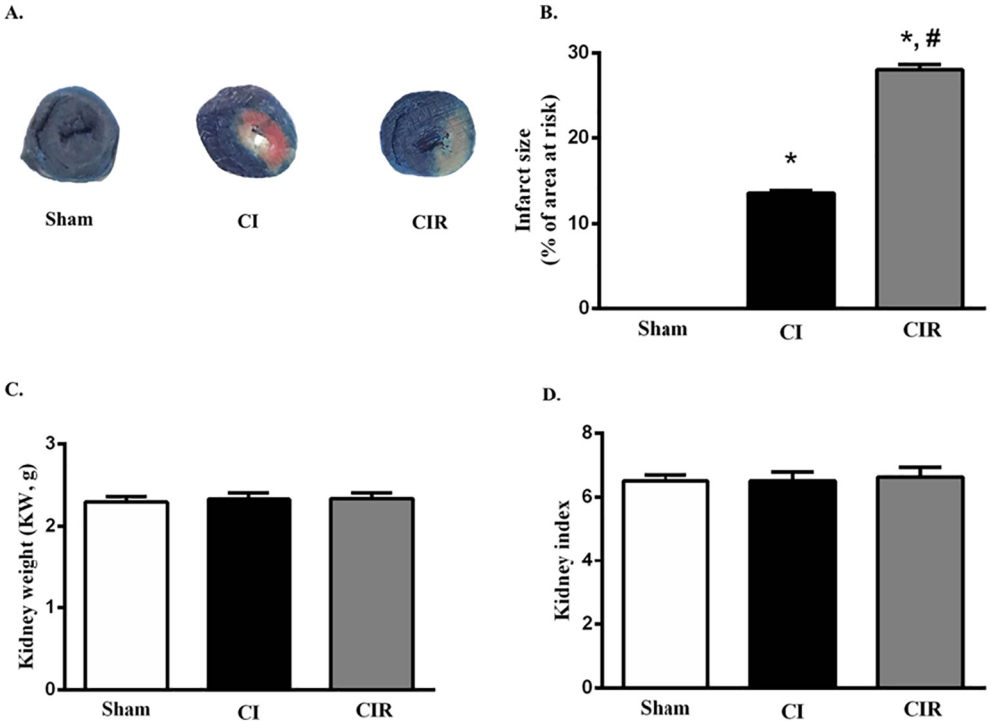

Fig. 1. Effect of acute cardiac ischaemia (CI) and cardiac ischaemia/reperfusion (CIR) on cardiac infarct size, kidney weight and kidney index. (A) Representative images of cardiac infarct area (no stained), viable area (red) and area at risk (no blue stained). (B) Cardiac infarct size is presented as percent of area at risk. (C) Kidney weight and (D) kidney index as calculated by kidney weight per body weight and multiplied by 1000. Data were expressed as mean ± S.E.M. (n = 6). *p < 0.05 vs sham group, #p < 0.05 vs CI group.

three times and the JC-1 monomer forms was determined at 520 nm excitation and 596 nm emission, while aggregate forms was determined at 485 nm excitation and 538 nm emission for green and red fluorescence, respectively. A decrease in the ratio of monomer to aggregate form represents mitochondrial depolarisation.

2.8. Quantitative real-time PCR analysis

Total RNA was purified from freshly isolated rat renal cortical tissues using trizol, according to the manufacturer's instruction. The first strand cDNA was obtained using iScript™ cDNA synthesis kit (Bio-rad, CA, USA) and qPCR was performed using SYBR green supermix. Primers were used according to published sequences (Table 1) and were purchased from Macrogen (Rockville MD). Gene expressions were normalised to actin mRNA levels and reported as relative fold changes (RFC). QPCR amplification was performed in duplicate for each cDNA.

2.9. Subcellular fractions and Western blot analysis

The renal cortical tissues in each condition were cut and suspended in CelLytic MT mammalian tissue lysis/extraction reagent containing 1% complete protease inhibitor. The samples were centrifuged at 5000 ×*g* for 10 min at 4 °C. Supernatant was specified as whole cell lysate and the pellet was re-suspended in the same lytic solution and centrifuged at 10,000 ×*g* for 10 min at 4 °C. The supernatant from this step was specified as the nuclei fraction. Whole cell lysate fraction was subsequently centrifuged at 100,000 ×*g* for 2 h at 4 °C and the supernatant was specified as the cytosolic fraction while the crude membrane pellets was re-suspended in the same reagent. Protein concentration of each sample was measured using Bradford assay (Bio-rad, CA, USA) and stored at −80 °C for further experiments. For Western blotting, protein sample was resolved in 2× Laemmli solution and electrophoresed on 10 or 15% SDS-PAGE, and subsequently transferred onto polyvinylidene difluoride (PVDF) membrane (Millipore, MA, USA). Non-

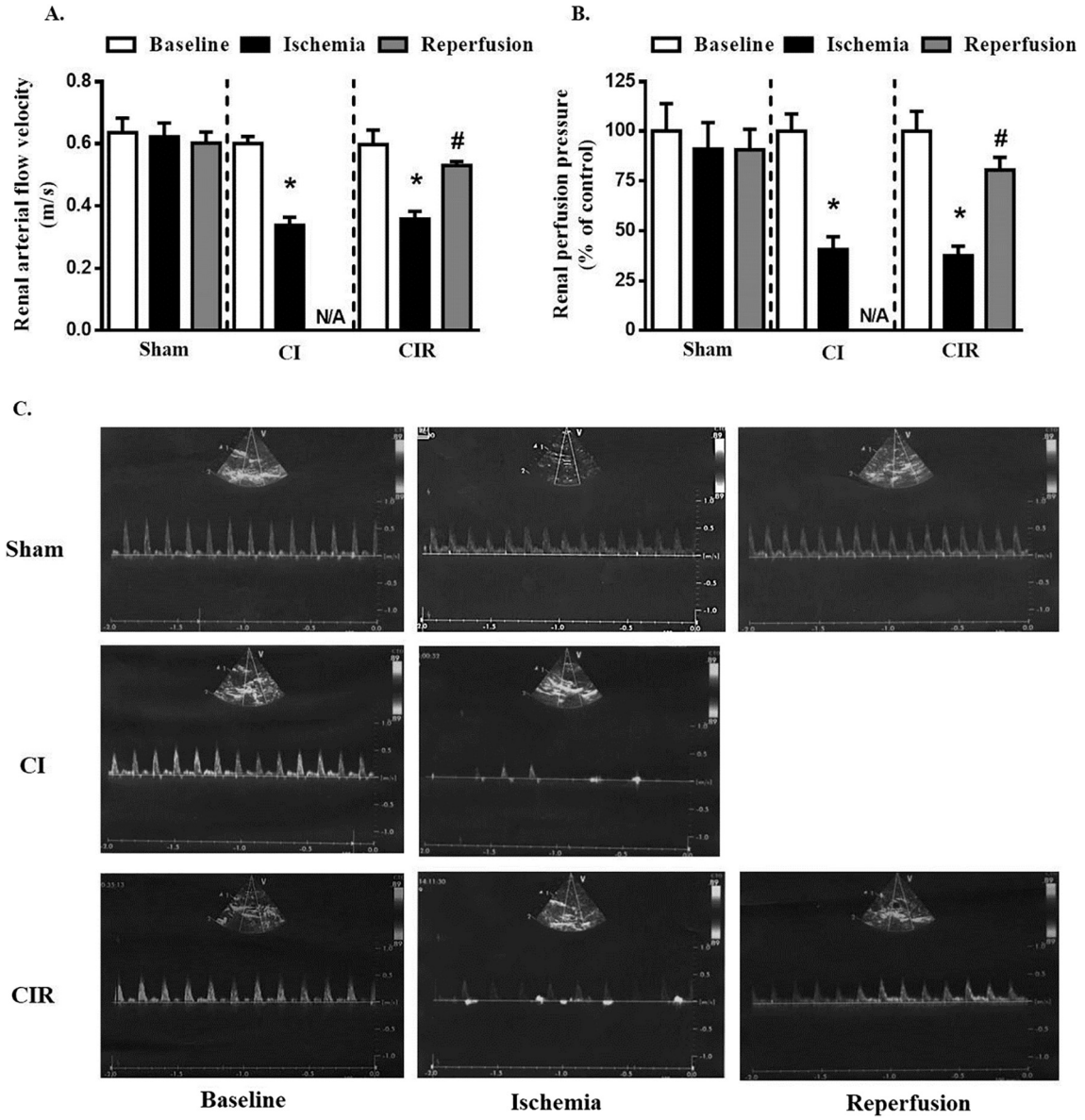

Fig. 2. Effect of cardiac ischaemic (CI) and cardiac ischaemic/reperfusion (CIR) conditions on renal arterial flow velocity and renal perfusion pressure. (A) Renal blood flow velocity, (B) relative renal perfusion pressure and (C) representative ultrasonic images in conditions during baseline (white bars), 15 min after ischaemia (black bars) and 15 min before end of reperfusion (grey bars). Data were expressed as mean ± S.E.M. (n = 6). *$p < 0.05$ vs respective baseline, $^{\#}p < 0.05$ vs CI group.

specific bindings of the protein on the membrane were blocked by 5% non-fat dry milk in 0.1% Tween 20 tris- or phosphate-buffered saline (TBST or PBST) for 1 h at 4 °C, then incubated overnight with the desired primary antibodies against rOat1, rOat3, PKCα, p-PKCα, PKCζ, p-PKCζ, Akt, p-Akt, p65NFκB, KIM1 and IL-18. To confirm the enrichment of the fraction, anti-Na^+-K^+-ATPase and anti-lamin B1 antibodies were used as membrane and nuclei markers, respectively. Anti-β-actin antibody was used as loading control for all samples. PVDF membranes were washed with TBST or PBST and incubated with goat anti-mouse, rabbit or goat IgG horseradish peroxidase-conjugated secondary antibody for 1 h at 4 °C. Enhanced chemiluminescent kit was utilised to detect the target proteins. The band density was quantitatively analysed by ImageJ program from Research Services Branch (RSB) of the National Institute of Mental Health (NIMH, MD, USA).

2.10. Statistical analysis

Data were expressed as mean ± S.E.M. Statistical differences were assessed using one-way analysis of variance, followed by LSD post-hoc test using SPSS version 23 (IBM Corp., NY, USA). Differences were considered to be significant when $p < 0.05$.

3. Results

3.1. General characteristics of acute cardiac ischaemia and cardiac ischaemia/reperfusion on cardiac infarct size, kidney weight and kidney index in rats

To confirm myocardial infarction, Evan blue dye staining was used to determine area of blood flow during ischaemia condition. The area at risk was not stained with Evan blue, whereas viable area was seen in red. The cardiac infarct size was indicated by white area. Similar to previous study [26], cardiac infarct size normalised by area at risk was progressively deteriorated in the area supplied by LAD, in both acute cardiac ischaemia (CI) and cardiac ischaemia/reperfusion (CIR) when compared with sham operation (Fig. 1A and B). Moreover, the infarct

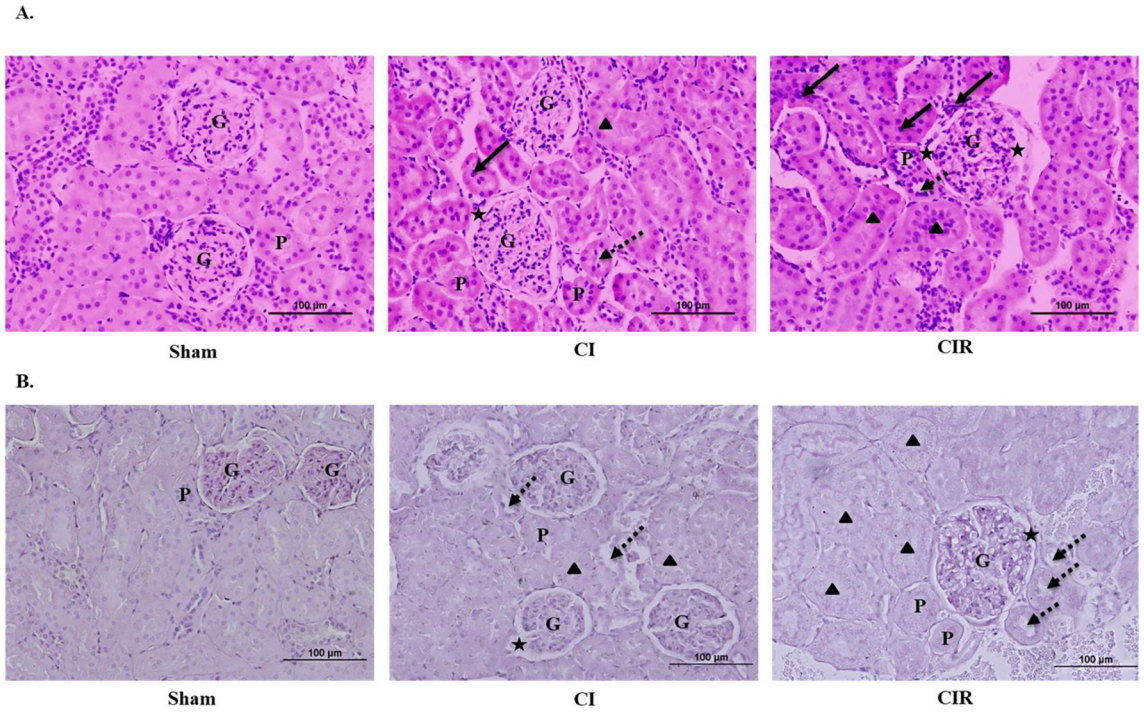

Fig. 3. Effects of acute cardiac ischaemia (CI) and cardiac ischaemia/reperfusion (CIR) on renal morphology. Representative micrographs of conventional (A) haematoxylin and eosin (H&E), and (B) periodic acid-Schiff base (PAS) staining of rat kidney section from sham, cardiac ischaemia (CI) and cardiac ischaemia and reperfusion (CIR) groups. Data were analysed from 6 areas in each slide section from 6 different animals using bright-field microscopy at 200×. * indicates wide Bowman's capsule space, → indicates nucleus condensation, ⇢ indicates brush border loss and ∇ indicates tubular dilatation. Abbreviations: G, glomerulus and P, proximal convoluted tubule.

area in the CIR group was greater than the CI alone. However, the kidney weight and index were not different among experimental groups (Fig. 1C and D). This data confirms that the LAD ligation protocol was reproducible and able to mimic myocardial ischaemic and I/R condition presented in a clinical setting.

3.2. Effects of acute cardiac ischaemia and cardiac ischaemia/reperfusion on renal arterial flow velocity and renal perfusion pressure

To determine cardio-renal communication, renal blood flow velocity and renal perfusion pressure after CI and CIR conditions were employed using non-invasive flow and pressure assessments using pulse wave viewed ultrasound system. As shown in Fig. 2A, renal arterial flow velocity was significantly decreased to 0.34 ± 0.06 and 0.36 ± 0.06 m/s during the ischaemic phase in both CI and CIR groups, respectively, when compared with their respective control (0.60 ± 0.05 and 0.60 ± 0.11 m/s). The sham operation was unchanged. However, the velocity during complete cardiac reperfusion in the CIR group was almost fully restored to 0.53 ± 0.03 m/s when compared to the baseline. Similarly, relative percentage of renal perfusion pressure during ischaemic phase was dropped to 37–40% relative to the respective baseline in both CI and CIR groups. The pressure in the CIR group was recovered to 80% during complete cardiac reperfusion phase (Fig. 2B). The representative ultrasonic images in baseline, ischaemia and reperfusion phase in sham, CI and CIR group were shown in Fig. 2C. These data suggest that complete coronary occlusion resulted in renal hypoperfusion and hypopressure, whereas complete reperfusion fully restored renal perfusion and pressure.

3.3. Effects of acute cardiac ischaemia and cardiac ischaemia/reperfusion on renal morphology, blood urea nitrogen, plasma creatinine and lipid peroxidation

Renal morphological analysis was assessed using standard methods for renal biopsy, haematoxylin & eosin and periodic acid-Schiff base (PAS) staining. Sham rat kidney had normal renal structures including the glomerulus, Bowman's capsule space and proximal convoluted tubules. On the other hand, CI and CIR rat kidney progressively developed glomerular infiltration with a wide Bowman's capsule space (star symbol), nucleus condensation (line arrow), brush border loss (dot arrow) and tubular dilatation (triangle symbol) (Fig. 3A and B).

Consistently, blood urea nitrogen (BUN) and plasma creatinine levels were elevated in CI rats and significantly increased in CIR rats when compared with sham (Fig. 4A and B). Similarly, plasma and renal cortical malondialdehyde levels, which represent lipid peroxidation, were higher in the CI group than the sham, while there was significant increase in the CIR rats when compared to the sham operation (Fig. 4C and D). These data indicate that acute myocardial ischaemic and I/R sequentially damage renal glomerular and tubular structures, and induce systemic and renal oxidative stress, which lead to progressive decline of renal function.

3.4. Effects of acute cardiac ischaemia and cardiac ischaemia/reperfusion on expression of antioxidants, pro-inflammatory cytokines and kidney injury markers

To identify the remote sensing and signalling mechanism by which CI and CIR affected renal tubular oxidative stress leading to renal dysfunction, renal antioxidant genes including superoxide dismutase (SOD), catalase (CAT) and glutathione peroxidase (GPx), extracted from renal cortical tissues, were assessed using quantitative real-time PCR. As shown in Fig. 5A, mRNA expression of a major mitochondrial ROS scavenging enzyme, manganese SOD (MnSOD), in renal tubular cells progressively decreased in CI and CIR. In addition, mRNA expression of cytosolic copper-zinc SOD (Cu-ZnSOD) and CAT in renal cortical tissues markedly decelerated in the CIR group when compared to the sham and CI groups, while GPx mRNA expression was abruptly, and continuously, blunted in CI and CIR conditions. Moreover, the dominant sources of

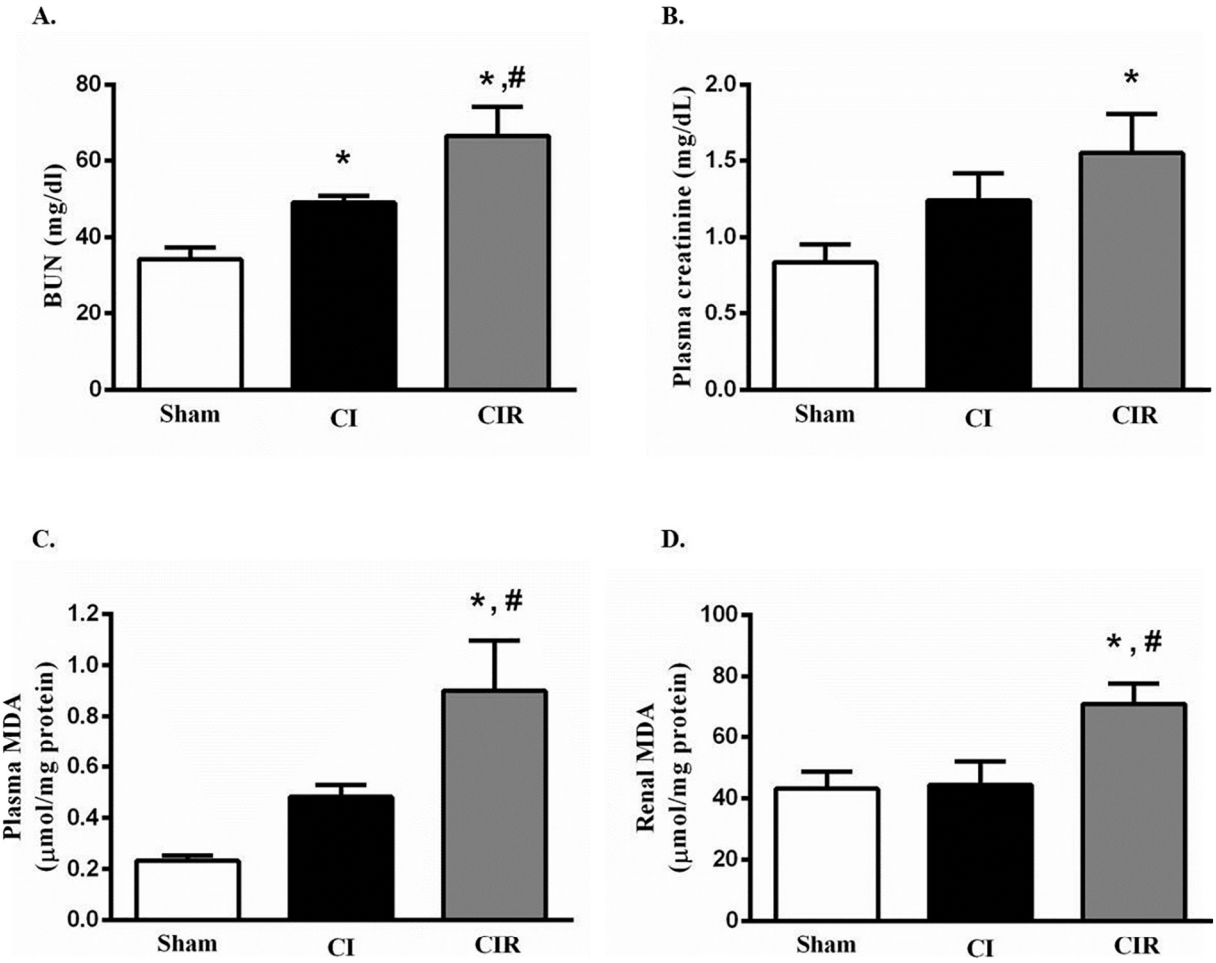

Fig. 4. Effect of cardiac ischaemia (CI) and cardiac ischaemia/reperfusion (CIR) on general renal function and oxidative stress. (A) Blood urea nitrogen (BUN), (B) plasma creatinine, (C) plasma malondialdehyde (MDA) and (D) renal cortical MDA levels. Data were analysed and expressed as mean ± S.E.M. (n = 6). *p < 0.05 vs sham, #p < 0.05 vs CI group.

ROS production including NADPH oxidase 2 (NOX2), NADPH oxidase 4 (NOX4) and xanthine oxidase (XO) mRNA expression in the CI group tended to increase when compared to the sham group. Expression of these three genes significantly increased the CIR condition when compared to the sham and CI groups (Fig. 5B).

Simultaneously, acute CI and CIR up-regulated mRNA expression of pro-inflammatory cytokines, including tumour necrosis factor-alpha (TNFα) and interleukin 1-beta (IL-1β) when compared to the sham group. Furthermore, cyclooxygenase 2 (COX2) mRNA expression was increased in the CIR group when compared to the sham and CI groups, while both CI and CIR up-regulated inducible nitric oxide synthase (iNOS) mRNA expression when compared to the sham group (Fig. 6A). Likewise, a significant expression of kidney injury molecule-1 (KIM-1) protein, a specific biomarker reflecting renal proximal tubular injury, was detectable in CI and CIR compared to the sham group (Fig. 6B), whereas IL-18 protein, a biomarker for early detection of AKI, was markedly increased in CIR compared to the sham group (Fig. 6C). These data suggest that CI and CIR can suddenly induce renal oxidative stress and inflammation and interfere cellular signalling processes, consequentially resulting in renal tubular injury.

3.5. Effects of acute cardiac ischaemia and cardiac ischaemia/reperfusion on renal mitochondrial structure and function

To further identify whether CI and CIR impaired redox state of renal tubular epithelial cells, renal mitochondria, a major source of active energy in renal tubules, was isolated. Its structure and function were subsequently determined. As shown in Fig. 7A and B, robust production of ROS was shown in the CI and CIR groups, in parallel with membrane depolarisation as reflected by the reducing renal mitochondria red/green JC1 ratio when compared with the sham group. CI and CIR condition also gradually induced renal mitochondria swelling when compared to the sham renal mitochondria (Fig. 7C). Consistently, protein expression of cleaved caspase 3, a downstream signalling marker of mitochondrial dysfunction, was higher and significantly increased in CI and CIR, respectively (Fig. 7D). Like functional changes, tubular mitochondrial content and tubular epithelium were gradually loss in CI and CIR, respectively, when compared to the sham condition (Fig. 7E). Similarly, isolated renal mitochondria in the sham group demonstrated nice and folded cristae in the inner membrane, while mitochondrial cristae extracted from CI and CIR gradually dispersed (Fig. 7F). This data indicate that sudden CI and CIR conditions have an instant remote sensing and signalling effect directed towards renal mitochondrial structure and function, which could potentially secrete kreb's cycle metabolites and key signalling molecules and impair active tubular function.

3.6. Effects of acute cardiac ischaemia and cardiac ischaemia/reperfusion on renal organic anion transport mediated by Oat1 and Oat3

We further identified the mechanisms by which CI and CIR directly impair active tubular function mediated by Oat1 and Oat3, the two potential new therapeutic targets for renal injury, using tubular transport study of organic anions in renal cortical slices. The [^{3}H]-PAH, a

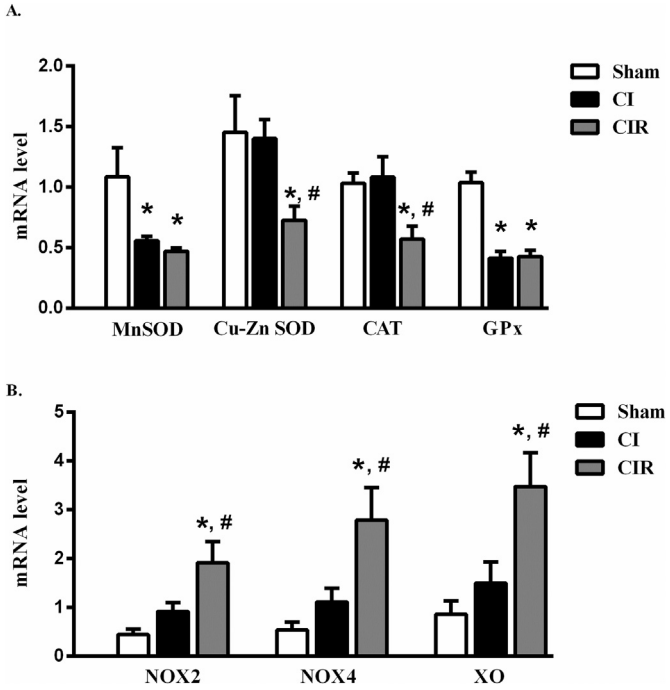

Fig. 5. Effect of cardiac ischaemia (CI) and cardiac ischaemia/reperfusion (CIR) on mRNA expression of antioxidants and oxidative stress gene. (A) Antioxidant enzymes, including manganese superoxide dismutase (MnSOD), copper-zinc SOD (Cu-ZnSOD), catalase (CAT) and glutathione peroxidase (GPx), and (B) oxidative stress gene markers, which are NADPH oxidases 2 (NOX2), NADPH oxidases 4 (NOX4) and xanthine oxidase (XO). Data were analysed and expressed as mean ± S.E.M. (n = 6). *p < 0.05 vs sham, #p < 0.05 vs CI group.

typical substrate for Oat1 and Oat3, and [^{3}H]-ES, a specific substrate for Oat3, were used in this experiment. As shown in Fig. 8A, PAH uptake was reduced in the renal slices of the CI group when compared to the sham group, while PAH transport mediated by Oat1 and Oat3 was markedly restored back after complete reperfusion, as seen in the CIR group. On the other hand, ES uptake mediated by Oat3 was not different among experimental groups (Fig. 8B). Consistent with functional transport, membrane protein expression of Oat1 was significantly down-regulated in the CI group compared to the sham group. Although Oat1 protein in the CIR group was markedly increased when compared to the CI group, it was still less expressed than that of the sham (Fig. 8C). Again, there was no significant difference in Oat3 membrane protein expression among experimental groups (Fig. 8D). These data indicate that among renal basolateral organic anion transporters, Oat1 is a major transporter that is susceptible to hypoperfusion and play a key target for pre-renal AKI which sequentially leads to impaired tubular transport function after myocardial infarction.

3.7. The mechanism involved in the impairment of renal organic anion transporter 1 induced by acute cardiac ischaemia and cardiac ischaemia/reperfusion

A study by Barros et al. [24] had shown that Oat1 and Oat3 functions shared a common trafficking process through insulin/PKCζ activation, leading to up-regulated Oat1 and Oat3 transport; whereas, our recent data showed that oxidative stress induced PKCα/NFkB activation, resulting in impaired Oat1 and Oat3 transport in type 2 diabetes mellitus (T2DM) [25]. Therefore, we further addressed whether regulatory function of Oat1 (and Oat3) was impaired under CI and CIR conditions using renal cortical slices pre-incubated with insulin. As expected, the renal cortical slices incubated by insulin had significantly increased in both [^{3}H]-PAH and [^{3}H]-ES transports in the sham group. In contrast, a common trafficking process of Oat1 and Oat3 by insulin stimulation was blunted in renal cortical slices transported by [^{3}H]-PAH and [^{3}H]-ES in both the CI and CIR group (Fig. 9A and B). To identify the mechanisms of impairment, Oat1 and Oat3 trafficking was further investigated by Western blot analysis. As shown in Fig. 9C, CIR progressively activated PKCα as indicated by increasing phosphorylated PKCα/PKCα ratio. Similarly, nuclear protein expression of p65 NFκB was significantly increased in the CIR group when compared to sham and CI groups (Fig. 9D). In addition, the positive regulator of Oat1 and Oat3, PKCζ, was in-activated in CIR condition compared to that of sham and CI, as indicated by a decrease of phosphorylated PKCζ/PKCζ ratio (Fig. 9E). This data was in parallel with a marked down-regulation of PKB/Akt, a downstream signalling protein of insulin/PKCζ (Fig. 9F). These data indicate that the regulatory proteins of Oat1 (and Oat3) are also sensitive to renal hypoperfusion and oxidative stress following CI and CIR, which subsequently impair tubular transport function and worsen acute kidney injury.

4. Discussion

The present study demonstrated the precise molecular mechanisms of AMI-induced renal hypoperfusion, oxidative stress, inflammation, mitochondria dysfunction and basolateral Oat1 transport function using a well-established cardiac ischaemia and reperfusion (I/R) injury model to mimic the clinical setting of AMI patients, as previously described [26].

Renal hypoperfusion is a major characteristic of pre-renal AKI [33]. This factor is revealed to be a critical criteria causing severe AKI in both experimental animal models and AMI patients [34]. In this study, renal hypoperfusion was clearly demonstrated by renal arterial flow velocity during 30 min of cardiac ischaemia (CI) using non-invasive sonographic technology, as modified from recent study [27]. As suggested, this feature is a better tool for early, robust and sensitive detection of the changes in renal hemodynamic status, compared to conventional histology and serum creatinine level in cisplatin-induced nephrotoxicity in rats [27]. Although renal hemodynamic parameters were fully recovered after 120 min of reperfusion in this study, the general renal function, histological appearance, oxidative stress, inflammation and renal secretory transport function were progressively deteriorated.

Clinically, increase in serum creatinine, decrease in glomerular filtration rate (GRF) and urine output are the major criteria used for defining AKI [1]. However, the prevalence of AKI after AMI still remains high to-date. Thus, the time pattern of systemic perturbation includes renal dysfunction after AMI is crucially defined for early preventive strategies. For better understanding the role of renal transporters in physiological and pathophysiological conditions in the future, establishing remote sensing and signalling system through gaining adequate time series data from time of perturbation to restoration is essential [13,35]. Here, we found that not only a progressive increase in serum creatinine and BUN was demonstrated in both 30-min ischemia and 30-min ischemia and 120-min reperfusion conditions, but generation of renal oxidative stress by MDA production and tremendous decrease of antioxidant genes (NOX2, NOX4 and XO) were also presented. Consistently, cardiac and renal I/R injuries in rats elevated plasma and renal MDA, as well as decreased antioxidant genes, respectively [36,37]. NOX2 plays a role in ventricular remodelling after myocardial infarction [38], while NOX4 up-regulates cardiac remodelling and dysfunction [39]. Additionally, both NOX2 and NOX4 are highly expressed in kidney and influence the redox status by producing $O_2^{\cdot}$ and its derivatives during several cellular events, including cell proliferation, cell death, inflammation and oxygen sensing [38,39]. Similarly, XO has been shown to play a role in producing ROS in renal I/R model in rats [40]. Taken together, imbalance of the redox state in renal cortical tissues could be an initial factor contributing to dyshomeostasis of intracellular renal metabolism and signalling, leading to renal dysfunction. Besides oxidative stress, up-regulated pro-inflammatory

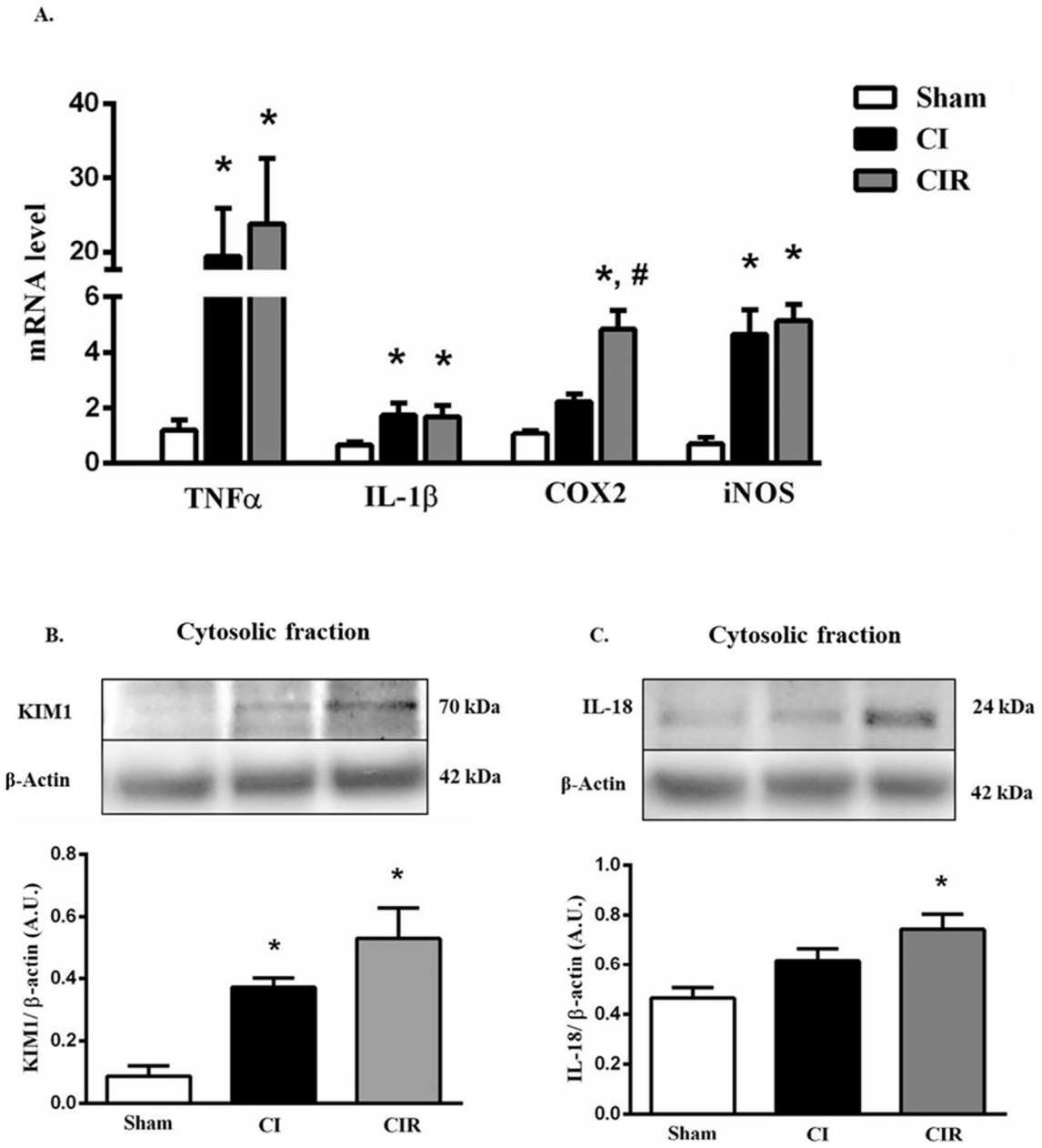

Fig. 6. Effect of cardiac ischaemia (CI) and cardiac ischaemia/reperfusion (CIR) on expression of pro-inflammatory cytokines mRNA and kidney injury protein markers. (A) Pro-inflammatory cytokines including tumour necrosis factor-alpha (TNF-α), interleukin-1β (IL-1β), cyclooxygenase-2 (COX2) and inducible nitric oxide synthase (iNOS), and (B) kidney injury protein markers, including kidney injury molecule-1 (KIM-1) and (C) interleukin-18 (IL-18). Representative blots of KIM-1 and IL-18 protein expression are shown in top panel, and quantification of relative proteins in cytosolic fraction are presented in bottom panel. Anti-KIM-1 and anti-IL-18 antibodies were detected while anti-β-actin antibody was used as loading control. Data were analysed and expressed as mean ± S.E.M. (n = 6). *$p < 0.05$ vs sham, $^{\#}p < 0.05$ vs CI group.

cytokines, which response to injury including TNF-α and IL-1β, have also been reported [41]. TNF-α is a potent pro-inflammatory cytokine that could promote tissue damage in AKI [42]. In addition, the key inflammatory enzymes, COX2 and iNOS, are also up-regulated in renal I/R [43]. In agreement with the line of evidences, partial hypoperfusion to the kidney by acute cardiac ischaemia and cardiac I/R in this study suddenly elevated TNF-α, IL-1β, COX2 and iNOS in renal cortical tissues. Consistently, the role of pro-inflammatory cytokines on interfering with Oat1 and Oat3 expression and function in several inflammatory diseases include sepsis and I/R injury has recently been discussed [44]. In addition, the greater the increase of plasma levels of urea with the greater the severity of pre-renal, nephrotoxic, and post-renal AKI, respectively [23]. Thus, renal cortical oxidative stress and inflammation due to acute cardiac ischaemia and cardiac I/R could contribute to the impairment of renal tubular transport function, in renal cortical nephrons. Although this study did not systemically measure specific uraemic toxins, endogenous metabolites from gut microbiome, nutrients, key small molecules, and antioxidants involved locally with renal dysfunction, our findings might imply that these molecules found in the blood circulation could potentially interfere renal tubular function, particularly during reperfusion phase. Further steps of investigations to describe the entire systemic consequences in inter-organ communication, especially, to seek the potential metabolites and signalling molecules release during sudden cardiac ischemic and I/R condition on renal transport function mediated by Oat1 in an in vivo are necessary. This could be done through metabolomic, transcriptomic, and/or

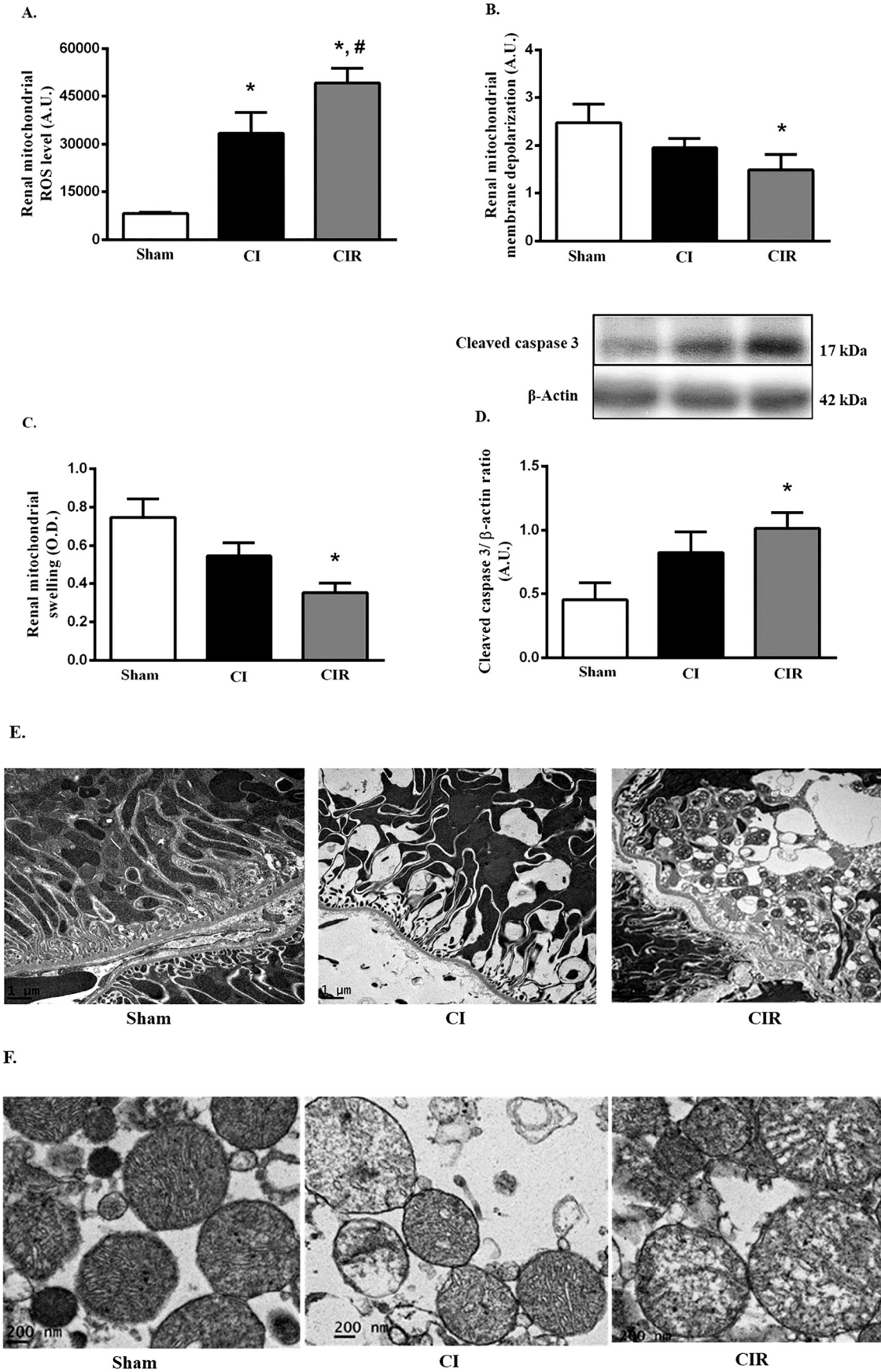

Fig. 7. Effect of cardiac ischaemia (CI) and cardiac ischaemia/reperfusion (CIR) on renal mitochondrial structure and function. The level of (A) ROS, (B) renal mitochondrial membrane depolarization and (C) renal mitochondrial swelling in isolated renal cortical mitochondria. (D) The cleaved caspase 3 expression, (E) mitochondrial content in renal tubular cells and (F) renal cortical mitochondrial morphology. Data were analysed and expressed as mean ± S.E.M. (n = 6). *$p < 0.05$ vs sham, $^{\#}p < 0.05$ vs CI group.

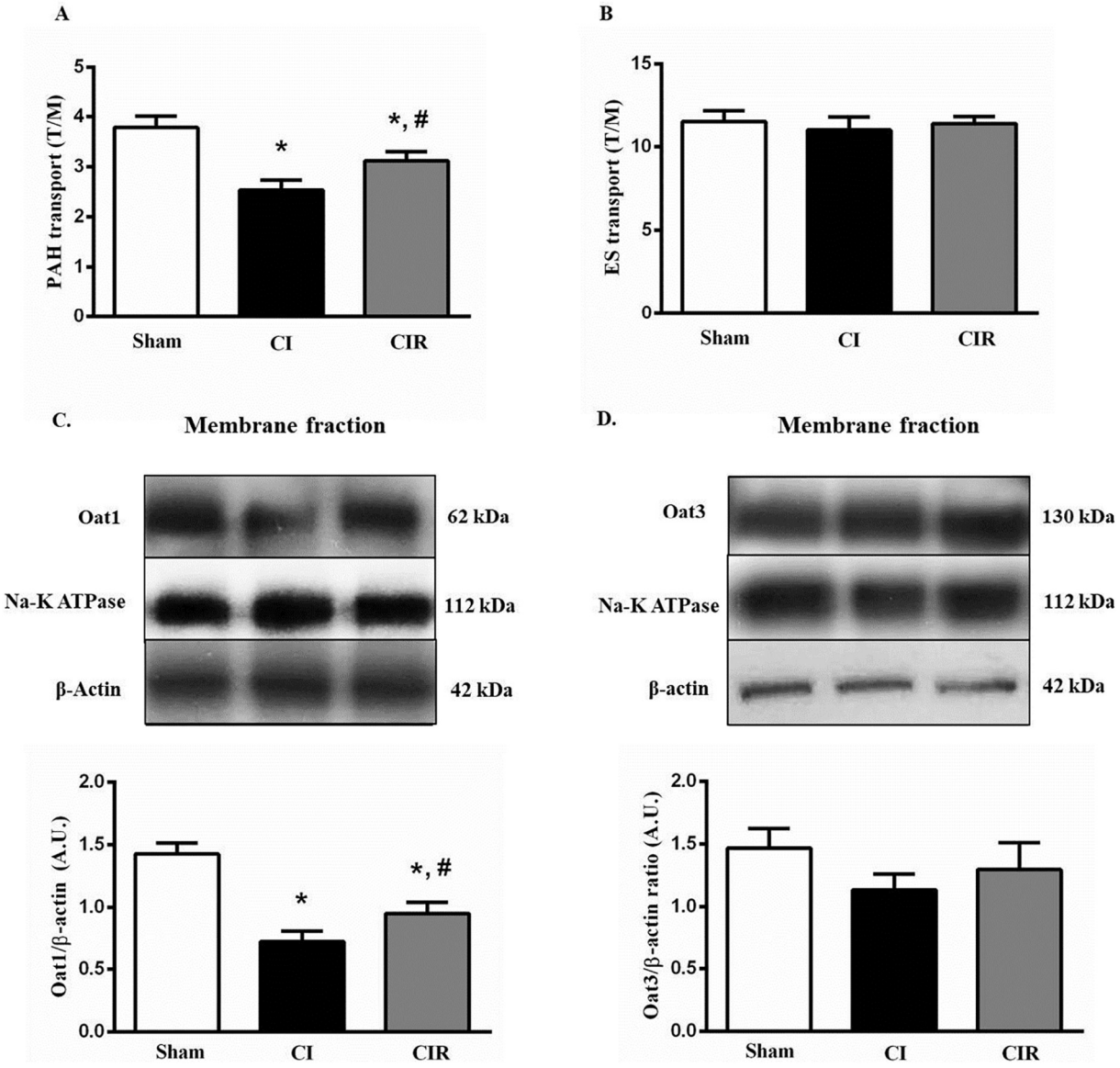

Fig. 8. Effect of cardiac ischaemia (CI) and cardiac ischaemia/reperfusion (CIR) on renal organic anion transport mediated by Oat1 and Oat3. (A) 5 μM [^{3}H]-PAH transport mediated by renal Oat1 and Oat3, and (B) 50 nM [^{3}H]-ES mediated by renal Oat3 for 30 min. Data were expressed as tissue to medium ratios (T/M), i.e. tissue content (DPM/mg) ÷ medium (DPM/μl) and represented as mean ± S.E.M. Each experiment was performed from separate animals, and at least three renal slices were used in each condition (n = 6). Renal tubular membrane expression of (C) renal organic anion transporter 1 (Oat1) and (D) renal organic anion transporter 3 (Oat3) were determined using specific anti-Oat1 and anti-Oat3 antibodies, respectively. Anti-Na^+-K^+-ATPase and anti-β-actin antibodies were used as membrane marker and loading control, respectively. Data were analysed and expressed as mean ± S.E.M. (n = 6). *$p < 0.05$ vs sham, $^{\#}p < 0.05$ vs CI group.

computational chemistry analyses.

Currently, patients who had myocardial infarction, organ transplant, surgical interventions, circulatory shock and haemorrhagic shock have gone through early detection of AKI by measuring major biomarkers, such as KIM-1 and IL-18 [45,46]. Again, our results indicated that these markers were significantly detected at only 30 min of occlusion and 120 min of reperfusion, implying that AKI could present even if only one episode of acute cardiac ischaemia and cardiac ischaemia/reperfusion had occurred. Thus, this study clearly demonstrates the heart-kidney communication in acute phenomenon, and a short window for prevention of pathological consequences of, particularly, cardio-renal syndrome type I remains necessary.

To further identify the impairment of renal tubular function, we investigate the mitochondria, as they are the major organelle for energy production that could also produce ROS, causing renal proximal tubular cell damage and apoptosis [47]. Furthermore, several evidences have shown that mitochondrial dysfunction could develop multiple organ failures, including the heart, liver, lung and kidney [48]. Previous study demonstrated that mitochondrial permeability transition pores (mPTPs) were closed during myocardial ischaemia [49]. On the other hand, these mPTPs were open at reperfusion phase, leading to induced ROS burst and increased Ca^{2+} and pH concentration in cardiac mitochondria [49]. As a consequent, cytochrome C is released and initiates the activation of the caspase cascade including caspase 3, leading to cell apoptosis [50]. Again, this study demonstrated that renal mitochondrial integrity and function were progressively destroyed after acute cardiac ischaemia and cardiac I/R injury. Since the secretory process in renal proximal tubule cells depends on ATP, the effects of acute cardiac ischaemia and cardiac I/R injury could possibly impair renal secretory function. To support this evidence, a very recent study revealed that tertiary active transport of Oat1 and Oat3 required higher amount of kreb's cycle metabolites, particularly α-ketoglutarate, in human conditionally immortalized proximal tubular epithelial cells overexpressing Oat1 and Oat3. Such process results in shifting cellular metabolism

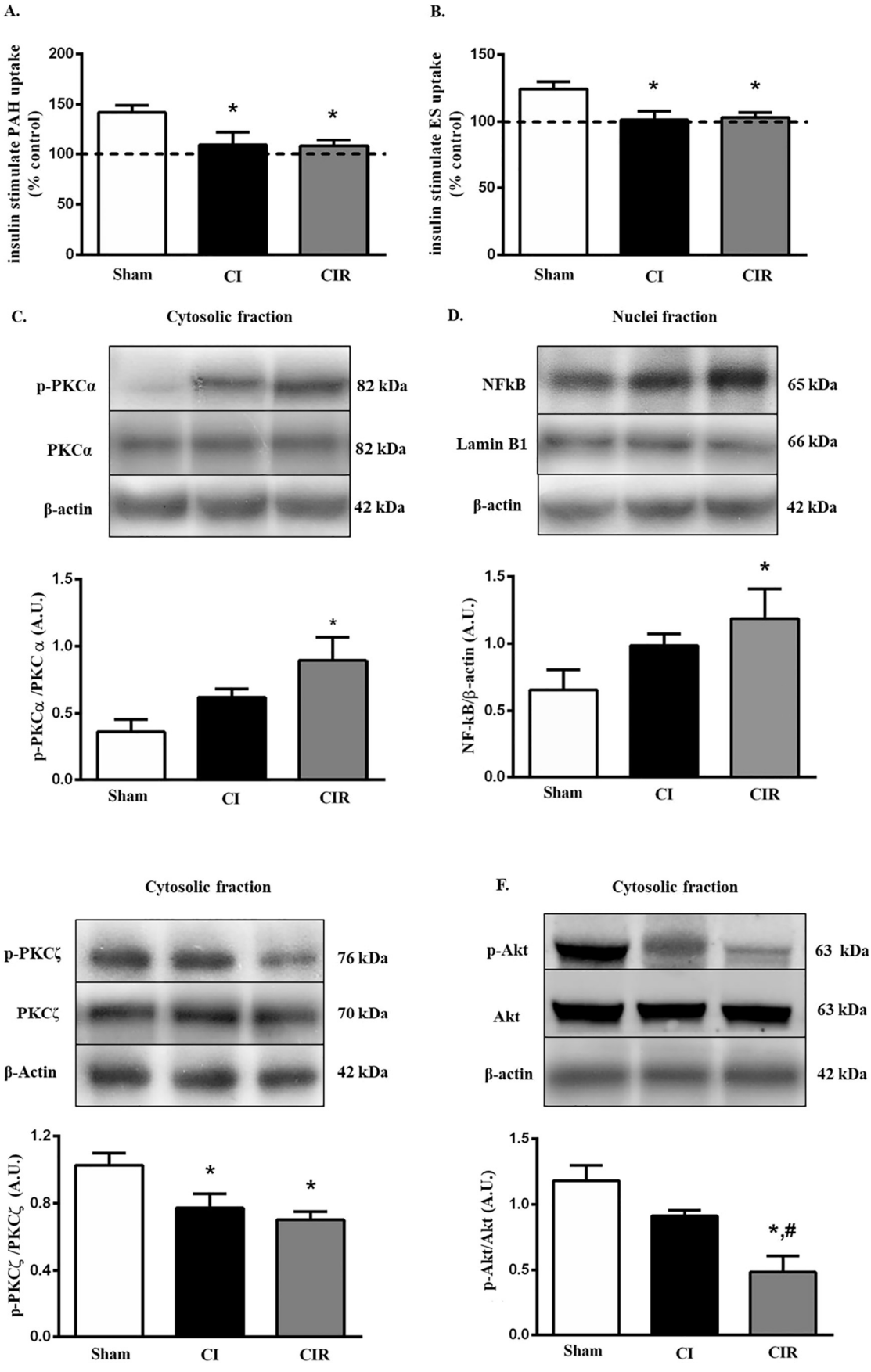

(caption on next page)

Fig. 9. Effect of cardiac ischaemia (CI) and cardiac ischaemia/reperfusion (CIR) on mechanism involved Oat1 and Oat3. The rat renal cortical slices were pre-incubated for 30 min in the presence or absence of 30 μg/mL of insulin, followed by (A) 5 μM [^{3}H]-PAH transport mediated by renal Oat1 and Oat3, and (B) 50 nM [^{3}H]-ES mediated by renal Oat3 for another 30 min. The data were analysed and expressed as % of mean control ± S.E.M. Each experiment was performed from separate animals, and at least 3 renal slices were used in each condition (n = 6). Renal tubular protein expression of (C) cytosolic p-PKCα and PKCα ratio, (D) nuclear p65 NFκB, (E) cytosolic p-PKCζ and PKCζ ratio and (F) cytosolic p-PKB/Akt and PKB/Akt were determined using specific antibodies. Anti-β-actin antibody was used as loading control. Data were analysed and expressed as mean ± S.E.M. (n = 6). *$p < 0.05$ vs sham, $^{\#}p < 0.05$ vs CI group.

towards oxidative state [51].

As Oat1 and Oat3 play a crucial role for the deterioration of kidney function, by accumulating uremic toxins derived from organ dysfunction [5], the set of common and overlapping substrates of Oat1 and Oat3 including uremic toxins and small metabolites were recently identified in Oat1 and Oat3 knock out mice by comparing against those substrates found in chemical double knock out model using metabolomic analysis. Evidence suggests that Oat1 and Oat3 play a role in endogenous metabolite disposition, metabolism, and excretion in healthy and pathological conditions [52]. Previously, the degree of rat Oat1 expression to be internalised into the cytosolic compartment in renal I/R model is time-dependent similarly to the human OAT1 expression in cadaveric renal allografts [53,54]. Correspondingly, the remote sensing effect of acute cardiac ischaemia in our study abruptly diminished functional Oat1 expression on the plasma membrane, while a 120-min reperfusion partially restored Oat1 impairment without changing the Oat3 expression and function. Hence, this study suggests that Oat1 is the major transporter susceptible to ischaemia and reperfusion-induced kidney injury. In addition, Oat1 might play a critical role in the pathological progression of cardio-renal syndrome (type I) through the remote sensing of cardio-renal communication. These findings strongly correlate with a more recent work which indicated that Oat1 is the centered-network in remote sensing and signalling by handling and regulating several metabolites and hormones e.g. kreb's cycle intermediates, indoxyl sulphate, prostagladins, and urea [8]. Indeed, bradykinin is found to be released under renal inflammation. This hormone has also up-regulated Oat3 function through PKCδ, PKCε and PKCζ [55]. Thus, the possibility of unchanged membrane Oat3 expression and function may be due to bradykinin release under cardiac ischaemic and I/R conditions, leading to compensatory response of Oat3 expression and function.

Despite previous studies characterising the distribution of Oat1/OAT1 under renal I/R [53,54], such findings did not investigate the mechanism by which Oat1/OAT1 were degraded, particularly during ischaemia. Hence, we examined the hypothesis of whether sorting or trafficking proteins involved impairment of Oat1 during ischaemia. Our previous studies demonstrated that insulin shares a common pathway for insertion with Oat1/Oat3 on the membrane through PKA/PKCζ, leading to a doubled function of these transporters [24]. Additionally, phorbol ester had been shown to down-regulate Oat1 expression and function through PKC [56], whereas insulin-stimulated Oat3 function in T2DM rat kidney was impaired by oxidative stress resulting in activation of PKCα/NFκB [25]. Likewise, the present study clearly demonstrated that insulin-stimulated Oat1/Oat3, through PKCζ/Akt, were depleted simultaneously with PKCα/NFκB activation during CI and CIR. These findings suggest that a sudden cardiac dysfunction can impair renal basolateral Oat1/Oat3 trafficking process, which could progressively reduce the net elimination of PAH and other organic anions, including uremic toxins which subsequently worsen kidney injury. To extend the line of Oat1 internalisation by PKC, a recent study also found that short-term PKC activation enhanced internalisation of Oat1 from plasma membrane to cytosol, while long-term PKC activation promoted the degradation of Oat1 via ubiquitin ligase Nedd4-2 [57].

Currently, the therapeutic treatments of AMI patients are mainly focused on the improvement of heart function using several agents including vasodilators, anti-coagulant, anti-platelet and antioxidants [58]. In addition, there are various pharmacological interventions that can restore renal function in renal I/R injury model, including ROS-scavenging agents, nitric oxide and NOS inhibitors, poly-ADP-ribose polymerase (PARP) inhibitors, peroxisome proliferator activated receptor (PPAR) agonists and adenosine receptor agonists [3]. Recently, indomethacin, an anti-inflammatory drug, has been shown to improve renal Oat1 and Oat3 in rat renal I/R model [59]. Since Oat1 is responsible for the clearance of endogenous metabolites and uraemic toxin [8], and in this study it was impaired after sudden CI, the therapeutic interventions targeting Oat1 and its regulatory proteins for patients who suffer from AKI induced by AMI should be crucially considered.

In conclusion, this promising study indicates that a sudden myocardial ischaemic and ischaemic/reperfusion conditions, can abruptly impair renal cortical mitochondria and basolateral transporters, particularly Oat1 and its regulatory proteins, which can, in turn, potentially worsen AKI. These findings, therefore, supports the remote sensing and signalling hypothesis of renal Oat1, and demonstrates an evidence of heart-kidney communication. Improving renal Oat1 and its regulatory proteins might be a useful therapeutic target for reversing such injury.

Transparency document

The Transparency document associated this article can be found, in online version.

Acknowledgements

This research was supported by the Thailand Research Fund [RSA5980009(CS), RSA6180056(SP)]; the Faculty of Medicine Endowment Fund, Faculty of Medicine, Chiang Mai University, Chiang Mai, Thailand [8/2562(CS)]; and the NSTDA Research Chair Grant from the National Science and Technology Development Agency (NC).

Declaration of competing interest

The authors declare that there is no conflict of interests regarding the publication of this paper.

References

[1] E. Kaltsas, G. Chalikias, D. Tziakas, The incidence and the prognostic impact of acute kidney injury in acute myocardial infarction patients: current preventive strategies, Cardiovasc. Drugs Ther. 32 (1) (2018) 81–98.
[2] C. Zoccali, D. Goldsmith, R. Agarwal, P.J. Blankestijn, D. Fliser, A. Wiecek, et al., The complexity of the cardio-renal link: taxonomy, syndromes, and diseases. Kidney Int Suppl (2011). 1 (1) (2011) 2–5.
[3] P.K. Chatterjee, Novel pharmacological approaches to the treatment of renal ischemia-reperfusion injury: a comprehensive review, Naunyn Schmiedeberg's Arch. Pharmacol. 376 (1–2) (2007) 1–43.
[4] P. Seth, R. Kumari, S. Madhavan, A.K. Singh, H. Mani, K.K. Banaudha, et al., Prevention of renal ischemia-reperfusion-induced injury in rats by picroliv, Biochem. Pharmacol. 59 (10) (2000) 1315–1322.
[5] S.H. Wright, W.H. Dantzler, Molecular and cellular physiology of renal organic cation and anion transport, Physiol. Rev. 84 (3) (2004) 987–1049.
[6] H. Koepsell, K. Lips, C. Volk, Polyspecific organic cation transporters: structure, function, physiological roles, and biopharmaceutical implications, Pharm. Res. 24 (7) (2007) 1227–1251.
[7] Pritchard JB MD. Proximal tubular transport of organic anions and cations. In: The Kidney: Physiology and Pathophysiology 2nd ed. ed. New York1992.
[8] H.C. Liu, N. Jamshidi, Y. Chen, S.A. Eraly, S.Y. Cho, V. Bhatnagar, et al., An organic anion transporter 1 (OAT1)-centered metabolic network, J. Biol. Chem. 291 (37) (2016) 19474–19486.
[9] Y. Miyamoto, H. Watanabe, T. Noguchi, S. Kotani, M. Nakajima, D. Kadowaki, et al., Organic anion transporters play an important role in the uptake of p-cresyl sulfate, a uremic toxin, in the kidney. Nephrology, dialysis, transplantation: official

publication of the European Dialysis and Transplant Association - European Renal Association. 26 (8) (2011) 2498–2502.
[10] H. Sun, L. Frassetto, L.Z. Benet, Effects of renal failure on drug transport and metabolism, Pharmacol. Ther. 109 (1–2) (2006) 1–11.
[11] T. Deguchi, Y. Kouno, T. Terasaki, A. Takadate, M. Otagiri, Differential contributions of rOat1 (Slc22a6) and rOat3 (Slc22a8) to the in vivo renal uptake of uremic toxins in rats, Pharm. Res. 22 (4) (2005) 619–627.
[12] S. Ohtsuki, H. Asaba, H. Takanaga, T. Deguchi, K. Hosoya, M. Otagiri, et al., Role of blood-brain barrier organic anion transporter 3 (OAT3) in the efflux of indoxyl sulfate, a uremic toxin: its involvement in neurotransmitter metabolite clearance from the brain, J. Neurochem. 83 (1) (2002) 57–66.
[13] W.R. Wikoff, M.A. Nagle, V.L. Kouznetsova, I.F. Tsigelny, S.K. Nigam, Untargeted metabolomics identifies enterobiome metabolites and putative uremic toxins as substrates of organic anion transporter 1 (Oat1), J. Proteome Res. 10 (6) (2011) 2842–2851.
[14] S.K. Nigam, K.T. Bush, Uraemic syndrome of chronic kidney disease: altered remote sensing and signalling, Nat. Rev. Nephrol. 15 (5) (2019) 301–316.
[15] A. Mónica Torres, M. Mac Laughlin, A. Muller, A. Brandoni, N. Anzai, H. Endou, Altered renal elimination of organic anions in rats with chronic renal failure, Biochim. Biophys. Acta (BBA) - Mol. Basis Dis. 1740 (1) (2005) 29–37.
[16] A. Enomoto, M. Takeda, A. Tojo, T. Sekine, S.H. Cha, S. Khamdang, et al., Role of organic anion transporters in the tubular transport of indoxyl sulfate and the induction of its nephrotoxicity, Journal of the American Society of Nephrology: JASN. 13 (7) (2002) 1711–1720.
[17] R. Schneider, C. Sauvant, B. Betz, M. Otremba, D. Fischer, H. Holzinger, et al., Downregulation of organic anion transporters OAT1 and OAT3 correlates with impaired secretion of para-aminohippurate after ischemic acute renal failure in rats, American journal of physiology Renal physiology. 292 (5) (2007) F1599–F1605.
[18] S.R. Villar, A. Brandoni, N. Anzai, H. Endou, A.M. Torres, Altered expression of rat renal cortical OAT1 and OAT3 in response to bilateral ureteral obstruction, Kidney Int. 68 (6) (2005) 2704–2713.
[19] H. Komazawa, H. Yamaguchi, K. Hidaka, J. Ogura, M. Kobayashi, K. Iseki, Renal uptake of substrates for organic anion transporters Oat1 and Oat3 and organic cation transporters Oct1 and Oct2 is altered in rats with adenine-induced chronic renal failure, J. Pharm. Sci. 102 (3) (2013) 1086–1094.
[20] Y. Sakurai, H. Motohashi, H. Ueo, S. Masuda, H. Saito, M. Okuda, et al., Expression levels of renal organic anion transporters (OATs) and their correlation with anionic drug excretion in patients with renal diseases, Pharm. Res. 21 (1) (2004) 61–67.
[21] C. Sauvant, H. Holzinger, M. Gekle, Prostaglandin E2 inhibits its own renal transport by downregulation of organic anion transporters rOAT1 and rOAT3, Journal of the American Society of Nephrology: JASN. 17 (1) (2006) 46–53.
[22] A.M. Torres, A.V. Dnyanmote, K.T. Bush, W. Wu, S.K. Nigam, Deletion of multispecific organic anion transporter Oat1/Slc22a6 protects against mercury-induced kidney injury, J. Biol. Chem. 286 (30) (2011) 26391–26395.
[23] A. Brandoni, A.M. Torres, Altered renal expression of relevant clinical drug transporters in different models of acute uremia in rats, Role of Urea Levels. Cellular physiology and biochemistry: international journal of experimental cellular physiology, biochemistry, and pharmacology. 36 (3) (2015) 907–916.
[24] S.A. Barros, C. Srimaroeng, J.L. Perry, R. Walden, N. Dembla-Rajpal, D.H. Sweet, et al., Activation of protein kinase Czeta increases OAT1 (SLC22A6)- and OAT3 (SLC22A8)-mediated transport, J. Biol. Chem. 284 (5) (2009) 2672–2679.
[25] A. Ontawong, N. Saowakon, P. Vivithanaporn, A. Pongchaidecha, N. Lailerd, D. Amornlerdpison, et al., Antioxidant and renoprotective effects of Spirogyra neglecta (Hassall) Kützing extract in experimental type 2 diabetic rats, Biomed. Res. Int. 2013 (2013).
[26] S. Palee, P. Weerateerangkul, K. Chinda, S.C. Chattipakorn, N. Chattipakorn, Mechanisms responsible for beneficial and adverse effects of rosiglitazone in a rat model of acute cardiac ischaemia-reperfusion, Exp. Physiol. 98 (5) (2013) 1028–1037.
[27] Fisch S, Liao R, Hsiao L-L, Lu T. Early detection of drug-induced renal hemodynamic dysfunction using sonographic Technology in Rats. Journal of Visualized Experiments: JoVE. 2016(109):52409.
[28] T.W. Tervaert, A.L. Mooyaart, K. Amann, A.H. Cohen, H.T. Cook, C.B. Drachenberg, et al., Pathologic classification of diabetic nephropathy, Journal of the American Society of Nephrology: JASN. 21 (4) (2010) 556–563.
[29] D.S. Kiss, I. Toth, G. Jocsak, A. Sterczer, T. Bartha, L.V. Frenyo, et al., Preparation of purified perikaryal and synaptosomal mitochondrial fractions from relatively small hypothalamic brain samples, MethodsX. 3 (2016) 417–429.
[30] M.R. Wieckowski, C. Giorgi, M. Lebiedzinska, J. Duszynski, P. Pinton, Isolation of mitochondria-associated membranes and mitochondria from animal tissues and cells, Nat. Protoc. 4 (11) (2009) 1582–1590.
[31] N. Apaijai, H. Pintana, S.C. Chattipakorn, N. Chattipakorn, Effects of vildagliptin versus sitagliptin, on cardiac function, heart rate variability and mitochondrial function in obese insulin-resistant rats, Br. J. Pharmacol. 169 (5) (2013) 1048–1057.
[32] S. Thummasorn, S. Kumfu, S. Chattipakorn, N. Chattipakorn, Granulocyte-colony stimulating factor attenuates mitochondrial dysfunction induced by oxidative stress in cardiac mitochondria, Mitochondrion. 11 (3) (2011) 457–466.
[33] K. Makris, L. Spanou, Acute kidney injury: definition, pathophysiology and clinical phenotypes, The Clinical biochemist Reviews. 37 (2) (2016) 85–98.
[34] M. Legrand, D. Payen, Understanding urine output in critically ill patients, Ann. Intensive Care 1 (1) (2011) 13.
[35] S.K. Nigam, K.T. Bush, G. Martovetsky, S.Y. Ahn, H.C. Liu, E. Richard, et al., The organic anion transporter (OAT) family: a systems biology perspective, Physiol. Rev. 95 (1) (2015) 83–123.
[36] D.P. Basile, M.D. Anderson, T.A. Sutton, Pathophysiology of acute kidney injury, Comprehensive Physiology. 2 (2) (2012) 1303–1353.
[37] J.V. Bonventre, A. Zuk, Ischemic acute renal failure: an inflammatory disease? Kidney Int. 66 (2) (2004) 480–485.
[38] M. Zhang, A. Perino, A. Ghigo, E. Hirsch, A.M. Shah, NADPH oxidases in heart failure: poachers or gamekeepers? Antioxid. Redox Signal. 18 (9) (2013) 1024–1041.
[39] M. Zhang, A.C. Brewer, K. Schroder, C.X. Santos, D.J. Grieve, M. Wang, et al., NADPH oxidase-4 mediates protection against chronic load-induced stress in mouse hearts by enhancing angiogenesis, Proc. Natl. Acad. Sci. U. S. A. 107 (42) (2010) 18121–18126.
[40] D.N. Granger, P.R. Kvietys, Reperfusion injury and reactive oxygen species: the evolution of a concept, Redox Biol. 6 (2015) 524–551.
[41] X. Hong, X. Zhao, G. Wang, Z. Zhang, H. Pei, Z. Liu, Luteolin treatment protects against renal ischemia-reperfusion injury in rats, Mediat. Inflamm. 2017 (2017) 9783893.
[42] A. Akcay, Q. Nguyen, C.L. Edelstein, Mediators of inflammation in acute kidney injury, Mediat. Inflamm. 2009 (2009) 137072.
[43] P.K. Chatterjee, N.S. Patel, E.O. Kvale, S. Cuzzocrea, P.A. Brown, K.N. Stewart, et al., Inhibition of inducible nitric oxide synthase reduces renal ischemia/reperfusion injury, Kidney Int. 61 (3) (2002) 862–871.
[44] M. Murray, F. Zhou, Trafficking and other regulatory mechanisms for organic anion transporting polypeptides and organic anion transporters that modulate cellular drug and xenobiotic influx and that are dysregulated in disease, Br. J. Pharmacol. 174 (13) (2017) 1908–1924.
[45] H. Wu, M.L. Craft, P. Wang, K.R. Wyburn, G. Chen, J. Ma, et al., IL-18 contributes to renal damage after ischemia-reperfusion, Journal of the American Society of Nephrology: JASN. 19 (12) (2008) 2331–2341.
[46] W.K. Han, V. Bailly, R. Abichandani, R. Thadhani, J.V. Bonventre, Kidney injury molecule-1 (KIM-1): a novel biomarker for human renal proximal tubule injury, Kidney Int. 62 (1) (2002) 237–244.
[47] C. Wang, R.J. Youle, The role of mitochondria in apoptosis*, Annu. Rev. Genet. 43 (2009) 95–118.
[48] D.B. Zorov, M. Juhaszova, S.J. Sollott, Mitochondrial reactive oxygen species (ROS) and ROS-induced ROS release, Physiol. Rev. 94 (3) (2014) 909–950.
[49] M.G. Perrelli, P. Pagliaro, C. Penna, Ischemia/reperfusion injury and cardioprotective mechanisms: role of mitochondria and reactive oxygen species, World J. Cardiol. 3 (6) (2011) 186–200.
[50] M.E. Shawgo, S.N. Shelton, J.D. Robertson, Caspase-mediated Bak activation and cytochrome c release during intrinsic apoptotic cell death in Jurkat cells, J. Biol. Chem. 283 (51) (2008) 35532–35538.
[51] J. Vriend, C.A. Hoogstraten, K.R. Venrooij, B.T. van den Berge, L.P. Govers, A. van Rooij, et al., Organic anion transporters 1 and 3 influence cellular energy metabolism in renal proximal tubule cells, Biol. Chem. (2019), https://doi.org/10.1515/hsz-2018-0446.
[52] W. Wu, K.T. Bush, S.K. Nigam, Key role for the organic anion transporters, OAT1 and OAT3, in the in vivo handling of uremic toxins and solutes, Sci. Rep. 7 (1) (2017) 4939.
[53] O. Kwon, W.W. Wang, S. Miller, Renal organic anion transporter 1 is maldistributed and diminishes in proximal tubule cells but increases in vasculature after ischemia and reperfusion, American journal of physiology Renal physiology. 295 (6) (2008) F1807–F1816.
[54] O. Kwon, S.M. Hong, K. Blouch, Alteration in renal organic anion transporter 1 after ischemia/reperfusion in cadaveric renal allografts, The journal of histochemistry and cytochemistry: official journal of the Histochemistry Society. 55 (6) (2007) 575–584.
[55] Li S, Duan P, You G. Regulation of human organic anion transporter 3 by peptide hormone bradykinin. J. Pharmacol. Exp. Ther. 2010;333(3):970–5.
[56] N.A. Wolff, K. Thies, N. Kuhnke, G. Reid, B. Friedrich, F. Lang, et al., Protein kinase C activation downregulates human organic anion transporter 1-mediated transport through carrier internalization, Journal of the American Society of Nephrology: JASN. 14 (8) (2003) 1959–1968.
[57] D. Xu, J. Zhang, Q. Zhang, Y. Fan, C. Liu, G.P.K.C. You, Nedd4-2 signaling pathway regulates the cell surface expression of drug transporter hOAT1, Drug metabolism and disposition: the biological fate of chemicals. 45 (8) (2017) 887–895.
[58] J. Herlitz, B. Wireklintsundstrom, A. Bang, A. Berglund, L. Svensson, C. Blomstrand, Early identification and delay to treatment in myocardial infarction and stroke: differences and similarities, Scandinavian journal of trauma, resuscitation and emergency medicine. 18 (2010) 48.
[59] R. Schneider, M. Meusel, B. Betz, C. Held, K. Moller-Ehrlich, M. Buttner-Herold, et al., Oat1/3 restoration protects against renal damage after ischemic AKI, American journal of physiology Renal physiology. 308 (3) (2015) F198–F208.